Recent developments on the UrQMD hybrid model

J. Steinheimer,[1,2,*] M. Nahrgang,[1,**] J. Gerhard,[1,***]
S. Schramm,[1,****] and M. Bleicher[1,2,*****]

[1] *Frankfurt Institute for Advanced Studies (FIAS), Frankfurt am Main, Germany*

[2] *Institut für Theoretische Physik, Goethe-Universität, Frankfurt am Main, Germany*

We present recent results from the UrQMD hybrid approach investigating the influence of a deconfinement phase transition on the dynamics of hot and dense nuclear matter. In the hydrodynamic stage an equation of state that incorporates a critical end point (CEP) in line with lattice data is used. The EoS describes chiral restoration as well as the deconfinement phase transition. We compare the results from this new equation of state to results obtained, by applying a hadron resonance gas equation of state, focusing on bulk observables. Furthermore we will discuss future improvements of the hydrodynamic model. This includes the formulation of chiral fluid dynamics to be able to study the effects of a chiral critical point as well as considerable improvements in terms of computational time which would open up possibilities for observables that require high statistics.

1. INTRODUCTION

Studying the reaction products of high energy heavy ion collisions one hopes to find experimental evidence for a deconfinement phase transition from hadronic matter to the Quark-Gluon Plasma (QGP) phase. Many observables have been presented over the last years. A common problem with such observables is that they usually cannot be interpreted in an unambiguous way. An important step towards a thorough understanding of heavy ion collisions is therefore the development of models that can be applied over a wide range of

* Electronic address: steinheimer@th.physik.uni-frankfurt.de
** Electronic address: nahrgang@th.physik.uni-frankfurt.de
*** Electronic address: jochen.gerhard@compeng.uni-frankfurt.de
**** Electronic address: schramm@fias.uni-frankfurt.de
***** Electronic address: bleicher@fias.uni-frankfurt.de

beam energies and that are able to describe as many observables as possible with as few parameters as needed.
In the following we will introduce such a model which allows for the straight forward introduction of a deconfinement and chiral phase transition in a hydrodynamic phase.

2. THE HYBRID MODEL

The UrQMD hybrid model is an integrated approach which combines the advantages of a hadronic transport approach with an intermediate hydrodynamical stage for the hot and dense phase of a heavy ion collision. The UrQMD Model [1, 2] (in its cascade mode) is used to calculate the initial state of a heavy ion collision for the hydrodynamical evolution [3]. This is done to account for the non-equilibrium dynamics in the very early stage of the collision. The coupling between the UrQMD initial state and the hydrodynamical evolution happens at a time t_{start} when the two Lorentz-contracted nuclei have passed through each other. At this start time all initial collisions have proceeded, i.e. also the initial baryon currents have decoupled from each other, and it is the earliest time at which local thermodynamical equilibrium may be achieved. To map all 'point-like' particles from UrQMD onto the spatial grid of the hydrodynamic model each hadron is represented by a Gaussian of finite width. This instantaneous thermalisation at t_{start} goes along with an increase in entropy, as entropy is maximized in the equilibrium state.

The full 3 + 1 dimensional ideal hydrodynamic evolution is performed using the SHASTA algorithm [4, 5]. The partial differential equations are solved on a three-dimensional spatial Eulerian grid with fixed position and size in the computational frame.

To transfer all particles back into the UrQMD model, an approximate iso-eigentime transition is chosen (see [6] for details). Here, we "freeze out" individual transverse slices, of thickness $\Delta z = 0.2$ fm, at a constant time-like transition hypersurface. This time for each slice is given, whenever the energy density ε, in every cell of this slice, has dropped below four times the ground state energy density (i.e. ~ 580 MeV/fm^3). This assures that all cells have passed through the mixed phase of the equation of state and the effective degrees of freedom at the transition are hadronic (see Fig. 1 for a depiction of this line of constant energy density in the T-μ_q phase diagram). By applying a gradual transition one obtains an almost rapidity independent switching temperature. The hydrodynamic fields, in

a given slice, are transformed to particle degrees of freedom via the Cooper-Frye equation on an isochronous time-like hypersurface in the computational frame (the hypersurface normal is $d\sigma_\mu = (d^3x, 0, 0, 0)$). In the present calculations, the total baryon number, the electric charge, the net strangeness and the total energy of the system are conserved exactly on an event-by-event basis.

After the particles are created according to our prescription, they proceed in their evolution in the hadronic cascade (UrQMD) where rescatterings and final decays are calculated until all interactions cease and the system decouples.

A more detailed description of the hybrid model including parameter tests and results can be found in [7].

Serving as an input for the hydrodynamical calculation the EoS strongly influences the dynamics of an expanding system. In the following we will present results for four different EoS and their effect on the extracted observables. The first EoS, named the hadron gas (HG), describes a non-interacting gas of free hadrons [8]. Included here are all reliably known hadrons with masses up to 2 GeV, which is equivalent to the active degrees of freedom of the UrQMD model (note that this EoS does not contain any form of phase transition). To model the deconfinement and chiral phase transitions we apply an hadronic flavor-SU(3) model, which is an extension of a non-linear representation of a sigma-omega model including the lowest-lying multiplets of baryons and mesons (for the derivation and a detailed discussion of the hadronic part of the model Lagrangian see [9–11]). In spirit similar to the PNJL model [12] it includes the Polyakov loop Φ as an effective field and it adds quark degrees of freedom. The temporal background field Φ is defined as $\Phi = \frac{1}{3}\mathrm{Tr}[\exp(i\int d\tau A_4)]$, where $A_4 = iA_0$ is the temporal component of the SU(3) gauge field (for details on the model see [13]). As can be seen in Fig. 1 the transition from hadronic to quark matter obtained is a crossover for small chemical potentials. At vanishing chemical potential the transition temperature is 171 MeV, determined as the peak of the change of the scalar field and the Polyakov loop. Beyond the critical end-point (at $\mu_{c,B} = 354$ MeV, $T_c = 167$ MeV for isospin symmetric matter in accordance with [14]) a first order transition line begins.

3. NUMERICAL RESULTS

Many bulk observables for a phase transition to a deconfined phase of QCD have been proposed over the last years. Due to the limited format of this paper we will exemplarily discuss two such observables.

Fig. 2 shows the excitation function of the mean transverse mass of different particles, at midrapidity. Especially for the pions one observes a good agreement with data for low energies. At high energies, both hydrodynamic calculations overestimate the mean transverse momenta, while the calculation with the DE EoS gives a slightly better description of the data still missing the data considerably. The flattening of the mean transverse momentum as a function of beam energy was assumed to be a signal for a first order phase transition [15]. But the slow increase of the mean transverse mass at increasing beam energy can be better related to non equilibrium effects, and may be modeled by the inclusion of viscous hydrodynamics.

Another observable that is deemed to be a signal for the deconfinement phase transition is the so called "anti-flow" (or third flow component). Data [16], indeed, show a wiggle in the directed flow in most central collisions at $E_{\rm lab} = 40$ AGeV. Fig. 3 shows v_1 of pions (circles) and protons (squares) as a function of rapidity (over y_b, the beam rapidity) for different model calculations, compared to data (green stars and diamonds). Here, we compare both hybrid model calculations (with and without a phase transition) and a pure transport calculation [17] (UrQMD without any hydrodynamic stage). As one can see all models yield very similar results and none can reproduce the behavior of the proton v_1. The pion v_1 is very well in line with data for both hydrodynamic calculations. Note that even the sign change for the pions as compared to protons is reproduced. Still, changing the EoS does not lead to distinguishable differences in the extracted directed flow. The directed flow seems to be mostly sensitive to the initial conditions and less to the subsequent hydrodynamical expansion.

4. CHIRAL FLUID DYNAMICS

Within a chiral fluid dynamic model we study critical fluctuations of a possible QCD phase transition by explicitly taking into account non-equilibrium effects [18]. As a low energy effective model of QCD we use the linear sigma model with quarks. In this model

chiral symmetry is explicitly broken and a phase transition between chirally broken and restored phase can be observed. The quark degrees of freedom are treated as a heat bath in local thermal equilibrium. The mesonic degrees of freedom of interest are the soft modes of the chiral fields coupled to the expansion of the quark fluid. By integrating out the latter we arrive at an effective potential of the chiral fields in presence of the quarks. We can then study different types and strengths of the phase transition by tuning the coupling between the quarks and the chiral fields.

Explicitly allowing for a non-equilibrium propagation of the chiral field ($\phi = \sigma, \boldsymbol{\pi}$), the classical equations of motion are:

$$\partial_\mu \partial^\mu \phi + \frac{\delta V_{\text{eff}}(\phi, T)}{\delta \phi} = 0\,. \tag{1}$$

Locally the chiral fields interact with the quark fluid and exchange energy and momentum. Within the 3 + 1 dimensional hydrodynamic description of the quarks we have to solve equations for energy and momentum conservation. For our studies we initialize an ellipsoidal shape of a high energy density. In the high energy density region chiral symmetry is approximately restored and the chiral fields are small while in vacuum they have a finite value. Gaussian initial fluctuations are then put on top of the fields and propagated as the system evolves. The subsequent non-equilibrium propagation of the chiral fields influences the fluid dynamic evolution of the quark fluid. Fig. 4 shows the time evolution of the energy density for a 2nd and 1st order phase transition. Since the relaxation times at a 2nd order phase transition become infinitely large, the system would need an infinite time for the critical fluctuations to form. Our non-equilibrium propagation thus limits the extend to which critical phenomena can be seen. As a consequence the evolution along a trajectory through the p.t. of 2nd order is rather smooth. At a first order phase transition the effective potential V_{eff} has two degenerate minima which are separated by a barrier. Non-equilibrium effects may cause regions where the chiral field stays in the unstable minimum while the system cools down. This leads to inhomogeneities of the energy density and formation of bubbles of higher energy densities, that move out of the center of the collision. This could be the basis for signatures of the critical point in heavy ion collisions.

5. REDESIGNING THE HYDRODYNAMIC SIMULATION SOFTWARE

The computational effort that is required for studies with the UrQMD hybrid model is considerably larger that that of default UrQMD transport model calculations. This puts an unnecessary constraint on studies that require large amounts of statistics. In the following we will outline a solution for this problem by rewriting parts of the software system from Fortran to C++ in order to use modern developments in computer architecture. In our new implementation we *avoid* as far as possible *memory lookups*, instead we *recalculate* quantities, where needed. Secondly we group *conditional jumps* according to their execution probability. Further, the new logical structure of the program decreases the number of *conditional jumps* massively. The interface to the Fortran parts of the program have been implemented in an extra interface header. In particular we switched completely to a single precision implementation wherever the loss of precision is negligible. We store data in *structs of arrays* (SOA) instead of *arrays of structs* (AOS). Because of the principle of superposition, different dimensions often do not influence. Hence when working on, e.g., a quantity in x-direction, neighbors of the datum are quickly accessed. In C++, we can make extensive usage of inline functions. We have substituted major part of the arrays, for intermediate values, by inline functions and hence avoided the memory lookup without loosing readability of the code. Finally, our simulation the EOS does not change during propagation time. Hence we decided create a base EOS-class and, by means of polymorphism, instantiate an EOS-object at the very beginning of the program. Therefore during the calculation of pressure and energy no conditional jumps are necessary – the calculation consists only of table lookups and scaling. Furthermore no conditional branches are needed to calculate border cells. We have introduced halo cells with special initial conditions such that the actual border cells are calculated via the same formulas as the rest of the grid.

6. CONCLUSION

We discussed the influence of chiral restoration and the deconfinement phase transition in a hybrid model calculation, comparing calculations for final particle properties in central AA collisions over a wide energy range to available data. Here either a hadron resonance gas EoS or the deconfinement EoS was applied. Regarding most observables both models give a reasonable description of data, without tuning any parameters of the model. We showed

that the observed flattening of $\langle m_T \rangle$ cannot be explained by a phase transition. Here other mechanisms, like viscosity and other non equilibrium effects play an essentially more important role, while the effect of the EoS on the directed flow is almost completely negligible. Introducing chiral dynamics in the hydrodynamical model, we showed that qualitative differences in the evolution of critical fluctuations can be seen, according to either a first or second order phase transition. In the future more computationally demanding studies are in order. Here an important step was taken by redesigned our program with respect to cache usage and control flow. By this means we could increase the speed by a factor grater than two, while we have reduced the memory consumption by a factor of five. Thus the number of simulated heavy ion events per hour of computer usage increases significantly. This can also be a first step to apply further acceleration techniques, such as the use of vectorization or the use of special code for accelerators. We implemented first SHASTA-Versions in *CUDA* and are now working on an *OpenCL* Version.

ACKNOWLEDGMENTS

This work was supported by HGS-hire and the Hessian LOEWE initiative through the Helmholtz International center for FAIR (HIC for FAIR). The computational resources were provided by the Frankfurt Center for Scientific Computing (CSC).

---

1. S. A. Bass *et al.*, Prog. Part. Nucl. Phys. **41**, 255 (1998).
2. M. Bleicher *et al.*, J. Phys. G **25**, 1859 (1999).
3. J. Steinheimer *et al.*, Phys. Rev. C **77**, 034901 (2008).
4. D. H. Rischke, S. Bernard, and J.A. Maruhn, Nucl. Phys. A **595**, 346 (1995).
5. D. H. Rischke, Y. Pursun, and J.A. Maruhn, Nucl. Phys. A **595**, 383 (1995).
6. Q. Li, J. Steinheimer, H. Petersen, M. Bleicher, and H. Stocker, Phys. Lett. B **674**, 111 (2009).
7. H. Petersen, J. Steinheimer, G. Burau, M. Bleicher, and H. Stocker, Phys. Rev. C **78**, 044901 (2008).
8. D. Zschiesche, S. Schramm, J. Schaffner-Bielich, H. Stoecker, and W. Greiner, Phys. Lett. B **547**, 7 (2002).
9. P. Papazoglou *et al.* Phys. Rev. C **59**, 411 (1999).

10. P. Papazoglou, S. Schramm, J. Schaffner-Bielich, H. Stoecker, and W. Greiner, Phys. Rev. C **57**, 2576 (1998).
11. V. Dexheimer and S. Schramm, Astrophys. J. **683**, 943 (2008).
12. K. Fukushima, Phys. Lett. B **591**, 277 (2004).
13. J. Steinheimer *et al.*, Phys. Rev. C **81**, 044913 (2010).
14. Z. Fodor and S. D. Katz, JHEP **0404**, 050 (2004).
15. L. Van Hove, Phys. Lett. B **118**, 138 (1982).
16. C. Alt *et al.* (NA49 Collab.), Phys. Rev. C **68**, 034903 (2003).
17. H. Petersen, Q. Li, X. Zhu, and M. Bleicher, Phys. Rev. C **74**, 064908 (2006).
18. K. Paech, H. Stoecker, and A. Dumitru, Phys. Rev. C **68**, 044907 (2003).
19. L. Ahle *et al.* (E866 Collab.), Phys. Lett. B **476**, 1 (2000).
20. C. Alt *et al.* (NA49 Collab.), Phys. Rev. C **77**, 024903 (2008).
21. S. V. Afanasiev *et al.* (NA49 Collab.), Phys. Rev. C **66**, 054902 (2002).

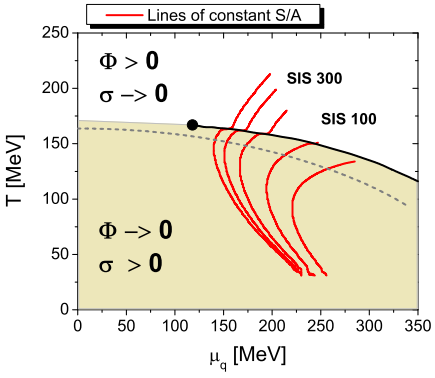

Figure 1. The line of the first order phase transition of the model, indicated in black together with the critical endpoint. Also shown is the line of constant energy density $\epsilon = 4\epsilon_0$ (gray dashed). The red lines show Isentropic expansion paths for very central PbPb/AuAu reactions at Beam energies: $E_{\rm lab} = 40, 30, 20, 10, 5$ AGeV.

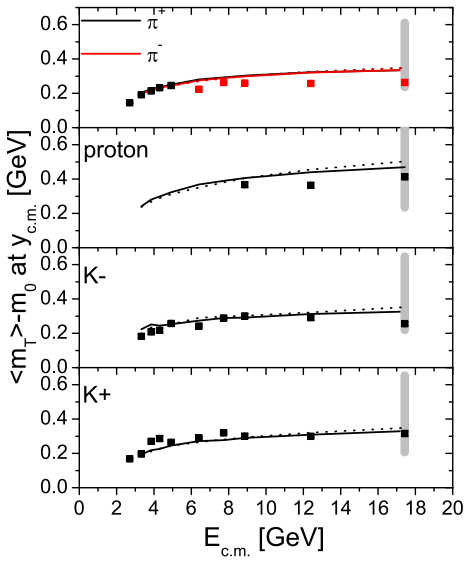

Figure 2. Excitation functions of the mean transverse mass of π (upper panel), protons (upper middle panel), K^- (lower middle panel) and K^+ (lower panel) with data [19–21].

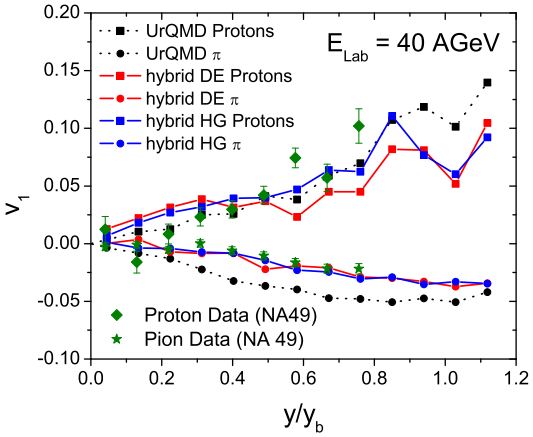

Figure 3. The directed flow v_1 for pions and protons at $E_{\rm lab} = 40$ AGeV for both hybrid model calculations (blue HG and red DE lines) compared to default UrQMD results (black dashed lines) and data (green stars and diamonds). y_b refers to the beam rapidity [16].

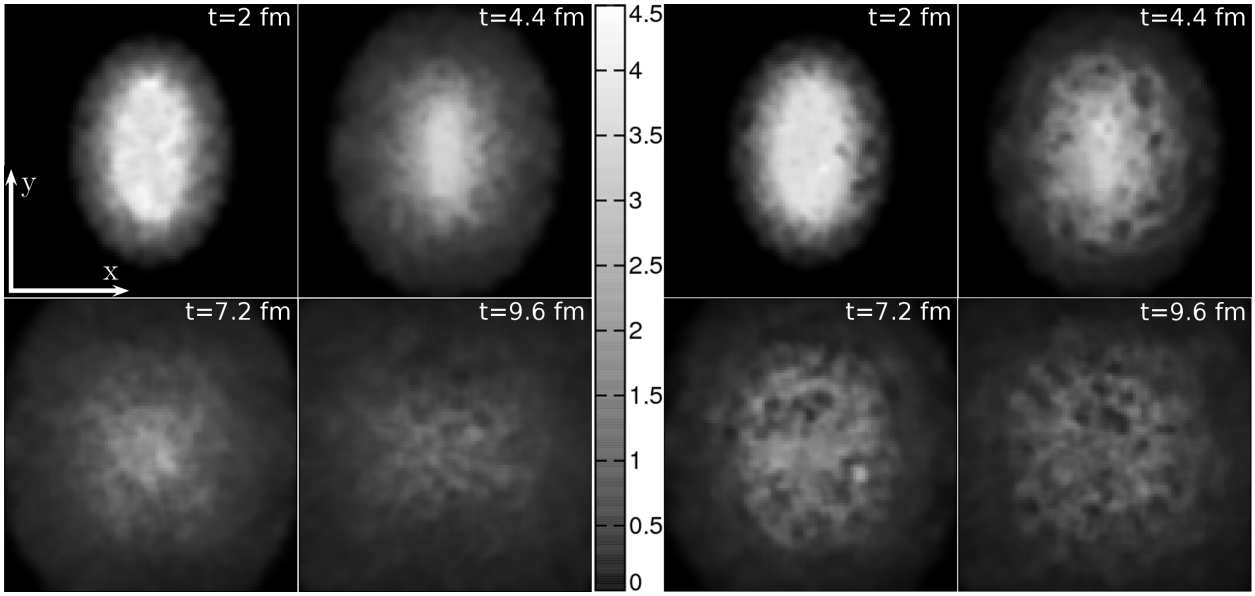

Figure 4. Energy density in units of $e_0 = 148$ MeV/fm^3 in the $x-y$-plane at $z = 0$ for a trajectory through a critical point (a) and through a first order phase transition (b).

FIGURE CAPTIONS

Fig. 1: The line of the first order phase transition of the model, indicated in black together with the critical endpoint. Also shown is the line of constant energy density $\epsilon = 4\epsilon_0$ (gray dashed). The red lines show Isentropic expansion paths for very central PbPb/AuAu reactions at Beam energies: $E_{\rm lab} = 40, 30, 20, 10, 5$ AGeV.

Fig.2: Excitation functions of the mean transverse mass of π (upper panel), protons (upper middle panel), K^- (lower middle panel) and K^+ (lower panel) with data [19–21].

Fig. 3: The directed flow v_1 for pions and protons at $E_{\rm lab} = 40$ AGeV for both hybrid model calculations (blue HG and red DE lines) compared to default UrQMD results (black dashed lines) and data (green stars and diamonds). y_b refers to the beam rapidity [16].

Fig. 4: Energy density in units of $e_0 = 148$ MeV/fm^3 in the $x-y$-plane at $z = 0$ for a trajectory through a critical point (a) and through a first order phase transition (b).